Acta Herpetologica 14(2): 117-122, 2019
DOI: 10.13128/a_h-7749

Ontogenetic and interspecific variation in skull morphology of two closely related species of toad, *Bufo bufo* and *B. spinosus* (Anura: Bufonidae)

Giovanni Sanna

Naturalis Biodiversity Center, P.O. Box 9517, 2300 RA Leiden, The Netherlands
Department of Biological, Geological, and Environmental Sciences, University of Bologna, Via Selmi 3, 40126 Bologna, Italy
Marine Research Department, Senckenberg am Meer, Südstrand 40, 26382 Wilhelmshaven, Germany
E-mail: giovanni.sanna3@studio.unibo.it

Submitted on: 2019, 31st January; Revised on: 2019, 6th June; Accepted on: 2019, 5th August
Editor: Marcello Mezzasalma

Abstract. Using micro-CT and 3D landmark-based geometric morphometrics, I investigated postmetamorphic shape variation in the skull of *Bufo bufo* and *Bufo spinosus*, two widespread European toad species with small phenotypic differences. Two ontogenetic series were compared, for a total of 58 individuals. They exhibited similar allometric growth patterns, characterised by cranial widening with relative shortening and dorsoventral compression. However, some interspecific shape divergence was observed, particularly among adults: a relatively shorter skull and a more dorsally extended snout distinguished *B. spinosus* from *B. bufo*. This disparity, which gives further support to species separation, can probably be ascribed to changes in the allometric trajectories, and seen in light of the evolutionary history of the two lineages.

Keywords. Allometry, *Bufo bufo*, *Bufo spinosus*, divergence, geometric morphometrics, landmark, ontogeny, skull shape.

INTRODUCTION

Divergent traits can be expected to be found in closely related species with a broad geographical distribution, relatively to ecological and climatic variation, but developmental constraints may also play an important role in restricting or channelling phenotypic evolution (Cvijanović et al., 2014; Ivanović and Arntzen, 2018). The Common toad, *Bufo bufo* (Linnaeus, 1758), and the Spined toad, *Bufo spinosus* Daudin, 1803, are members of the Common toad species group of the western Palaearctic (Arntzen et al., 2013b). *B. bufo* has a wide Eurasian distribution that comprises northern and eastern France, central and southern Europe (including Sardinia; Cossu et al., 2018), and stretches northwards into Scandinavia and eastwards deep into Russia; *B. spinosus* is found in the Iberian Peninsula, western and southern France, and North Africa, from Morocco to Tunisia (Arntzen et al., 2013a). Their lineages have diverged around 9 Ma (million years ago; Recuero et al., 2012), but in contrast to a deep genetic differentiation, *B. bufo* and *B. spinosus* appear phenotypically similar (Arntzen et al., 2013a). Whereas a few diagnostic characters were described for the external morphology, virtually nothing is known about interspecific osteological differences, neither in the postcranial nor in the cranial skeleton. Such a complex structure as the skull is of particular interest in a wide range of studies, due to its fundamental biological functions and the fact that it often undergoes adaptive variation (Ivanović et al., 2012). Substantial changes are

ISSN 1827-9635 (print)
ISSN 1827-9643 (online)

known to occur in the anuran skull after metamorphosis (Ponssa and Candioti, 2012).

The purpose of this investigation was to highlight potential interspecific differences in the skull morphology of *B. bufo* and *B. spinosus*, in the context of postmetamorphic development, using a geometric morphometrics approach. The analysis of ontogenetic shape variation in these two species is interesting not only for a taxonomic evaluation based on morphology; it can provide insights into their morphological evolution, to be interpreted in the context of their evolutionary history and past distribution. Moreover, this analysis could contribute to a better understanding of the interplay between ontogeny and morphological differentiation among anuran species.

MATERIAL AND METHODS

A total of 58 alcohol-stored specimens, including freshly metamorphosed, juvenile, and adult (male and female) toads, were analysed (Table S1). These toads had been collected from various populations in different localities of the Iberian Peninsula (*B. spinosus*), France (*B. spinosus*, *B. bufo*), and the Netherlands (*B. bufo*). They were subdivided into two ontogenetic series, made up of 28 *Bufo bufo* and 30 *Bufo spinosus* individuals, respectively. Body size in the whole sample ranged from 16.0 mm to 78.0 mm SUL (snout-urostyle length).

Mature *B. spinosus* individuals were larger on average (mean SUL 71.5 mm) than *B. bufo* ones (mean SUL 60.4 mm), reflecting size disparity between western European Common toads and Spined toads (Cvetković et al., 2009).

Three-dimensional imaging

Skulls were CT-scanned with two x-ray machines: SkyScan 1172 (Bruker, Kontich, Belgium) and ZEISS Xradia 520 Versa (Carl Zeiss XRM, Pleasanton, CA, USA). The former was used for the smaller toads, with 0.5 mm Aluminium filter, 2K resolution (2000 × 1336), pixel size of 13.17 μm, voltage of 29-54 kV, exposure time of 420-750 ms, 0.4 rotation step, averaging of four frames. Voltage and exposure time were modified when scanning specimens of different sizes (which showed differences in skull density), in order to keep image quality consistent. Xradia scanner was employed for adult individuals, mainly due to its larger sample holder; resolution was set at 1K (1000 × 1024), with pixel size of 34.18 μm, and voltage of 80 kV.

Scanning was followed by two-dimensional reconstruction of raw image data into stacks, which were processed with Avizo 9 software (FEI SAS, France): the segmentation editor was used to segregate homogeneous volumes (corresponding to skull bones), with manual adjustment of masking. Notable variation in the extent of cranial ossification, not merely restricted to small juveniles, was observed at this point. A 3D surface model of the skull was then generated, applying a variable degree of unconstrained smoothing according to ossification extent.

Landmarks

Thirty-one homologous landmark points were collected on each 3D surface model to describe overall skull shape (Fig. 1), using Landmark editor 3.6 (Institute for Data Analysis and Visualization, University of California, Davis, 2007). Fifteen points were bilateral and symmetric, while one was median. Anatomical description of points is provided in Table S2. Incomplete skull ossification of small juveniles made it challenging, at times, to perform an accurate placement of homologous landmarks (Zelditch et al., 2004).

Geometric morphometrics

Morphometric and statistical analyses based on the landmark coordinates, and qualitative observation of the associated shape changes, were carried out with MorphoJ 1.06 software (Klingenberg, 2011). A generalized Procrustes analysis (GPA), consisting of a full Procrustes superimposition for object symmetry, was applied: the symmetric components of shape variation, as a measure of skull shape, and centroid size, as a measure of skull size, were computed for each individual (Klingenberg, 2016). The covariance matrix of shape variables was then generated and used to perform a principal component analysis (PCA), in order to explore overall patterns of shape variation.

Shape changes in relation to growth were evaluated with a multivariate regression of shape (symmetric components, i.e. dependent variables) on size (log-transformed centroid size, i.e. independent variable), one for each ontogenetic series (Monteiro, 1999), in association with a permutation test against independence between dependent and independent variables (made up of 10^4 randomization rounds). The angle between the two regression vectors was calculated for comparison, including a test against randomness of vector directions in shape tangent space.

Interspecific morphological distinction was assessed by performing a discriminant function analysis (DFA) with leave-one-out cross-validation (Lachenbruch, 1967; Webster and Sheets, 2010) on shape data of the 25 largest individuals, 12 *B. bufo* and 13 *B. spinosus* toads comprising adults and subadults. Such a subsample was selected in order to maximize interspecific differences, since the PCA had previously shown shape divergence in late stages of growth (Fig. 2). Results of this analysis were compared with those of a DFA on the remaining individuals of the sample, namely juveniles. Both analyses included a parametric T-square test against the null hypothesis of equal group means, and a permutation test for the T-square statistic with 10,000 randomization rounds.

RESULTS

The first two principal components (PC1, PC2) of the PCA accounted for 71.9% of total shape variation. PC1 alone grouped 65.4% of variation and was positively correlated with size: therefore, the scatter plot of PC2

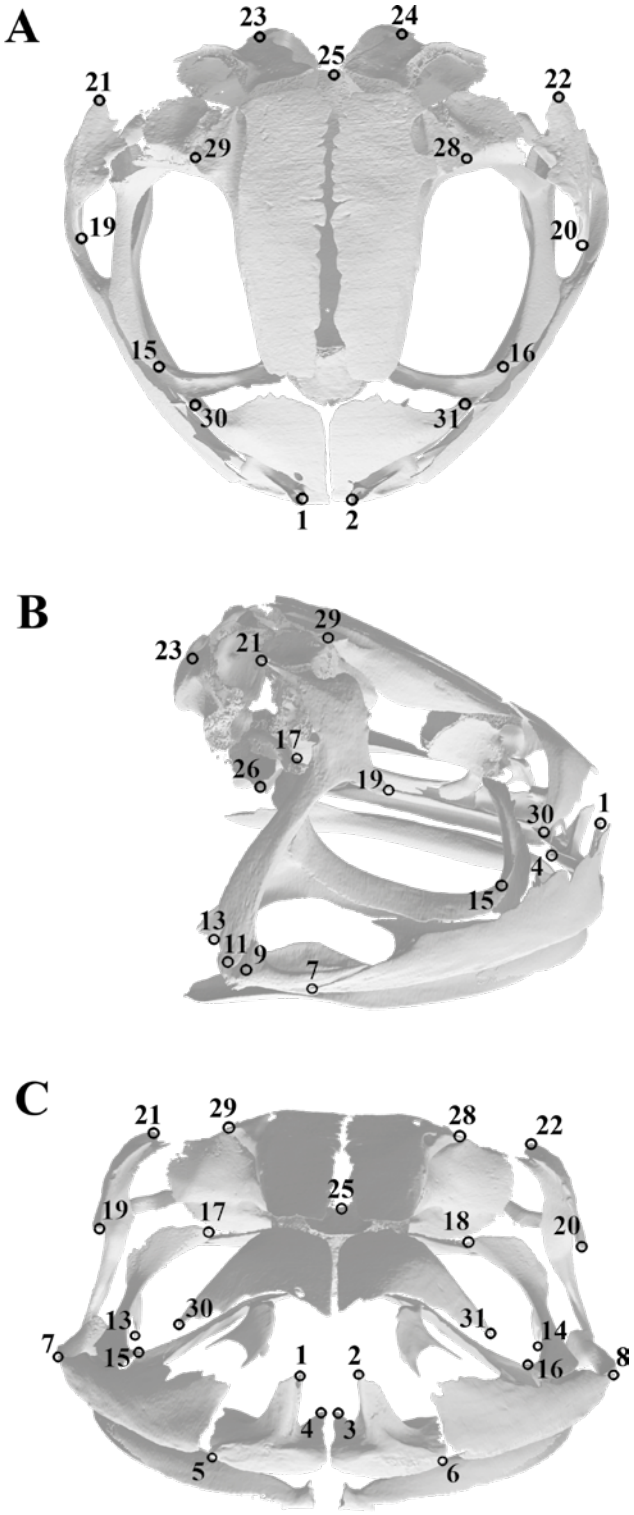

Fig. 1. Landmark positions on the digitized skulls, in dorsal (A), right lateral (B), and frontal (C) views. For the anatomical description of landmarks, see Table S2.

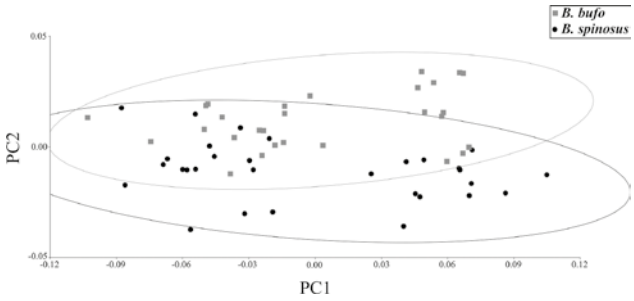

Fig. 2. Ontogenetic shape variation of *B. bufo* and *B. spinosus*, described by the scatter plot of the first two principal components (with 95% confidence ellipses). PC1 summarises allometric variation, while PC2 displays species divergence in late development.

vs. PC1 can be looked at as a morphospace that contains the ontogenetic shape trajectories of *B. bufo* and *B. spinosus* (Fig. 2). Cranial shape variation along PC1 was characterised, in the positive direction, by a broadening (at the level of the jaw joint), an overall shortening (at the level of both the exoccipital and the premaxilla), and dorsoventral compression. Some interspecific variation was comprised in PC2, especially for the largest toads; positive direction shape changes along this axis were an increase in skull length, dorsoventral compression, and a slight widening.

Both regression analyses found a significant association between shape and size ($P < 0.0001$ for both), indicating allometric growth: 63.8% of shape variation in *B. bufo* and 68.5% of shape variation in *B. spinosus* were predicted by regression on size (Fig. 3). The two vector directions formed an angle of 17.2° (whereas 0° denote complete correspondence, 90° maximum divergence) and were not random in the shape tangent space ($P < 0.00001$). The major shape changes associated with regression were corresponding between the two species and matched those related to the first principal component of the PCA, thus confirming the correlation of PC1 with skull size.

Discriminant function analysis applied to the largest toads showed a clear distinction between the two species (Fig. 4): after cross-validation, 10/12 *B. bufo* individuals were reassigned to their true group and 2/12 were allocated to the Spined toad group, while 13/13 *B. spinosus* individuals were reassigned to their own group (Cohen's $K = 0.84$). However, the T-square test for the difference between group means was not statistically significant ($T^2 = 281$, $P = 0.82$). Permutation produced a significant result instead ($P < 0.0001$). The major interspecific shape differences pointed out by the analysis concerned cranial length and height: *B. spinosus* exhibited a longer upper jaw (with a more posterior jaw joint), yet a shorter

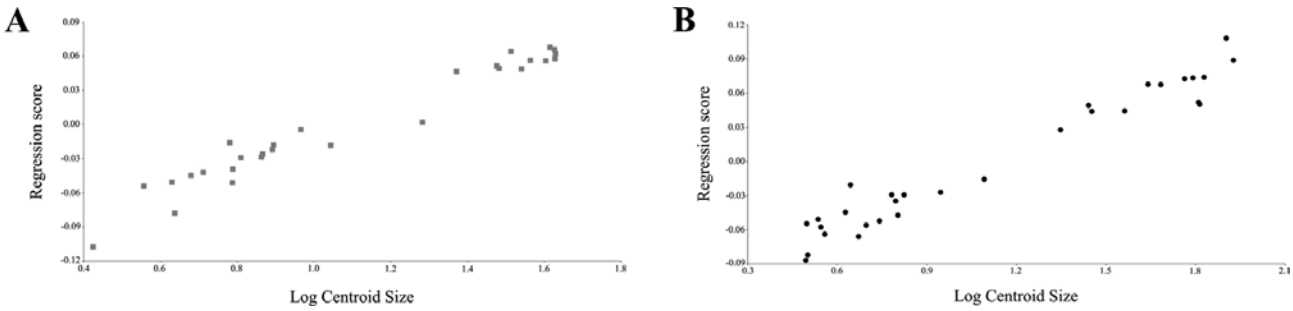

Fig. 3. Shape changes of *B. bufo* (A) and *B. spinosus* (B) in relation to size, described by the scatter plot of regression scores against log-transformed centroid size.

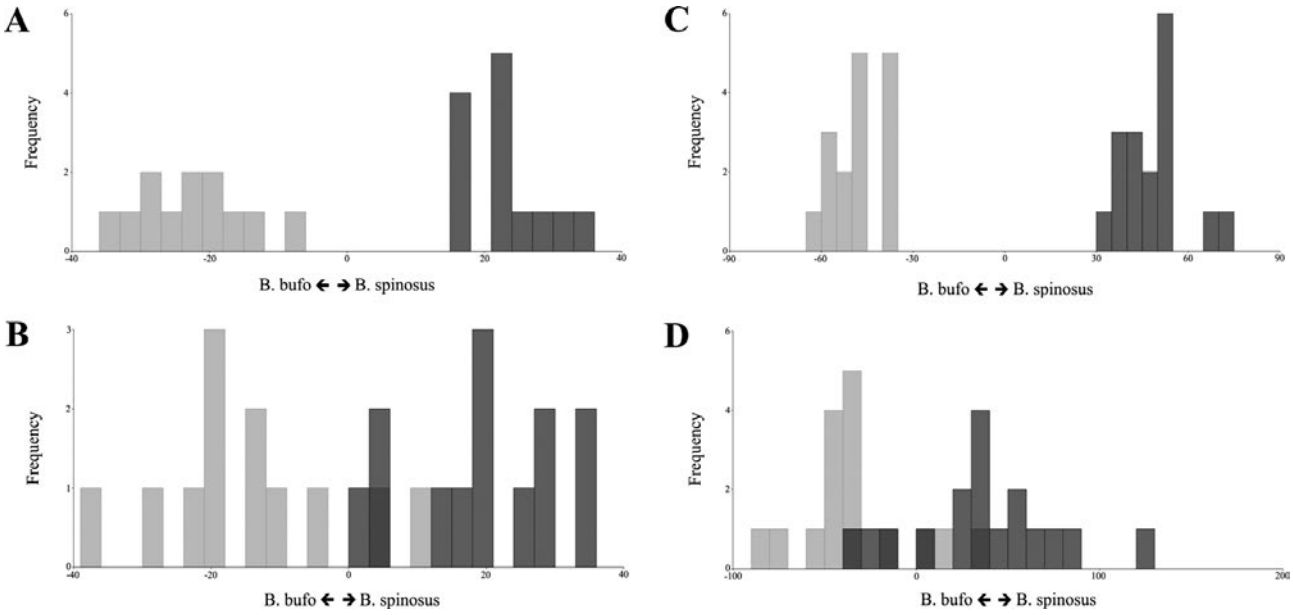

Fig. 4. Interspecific distinction, described by DFA histograms in which light grey bars represent *B. bufo* and dark grey bars represent *B. spinosus*. Species assignment and discriminant scores are shown before (A, C) and after (B, D) cross-validation, for the largest individuals (A, B) and juveniles (C, D).

skull (due to a shorter occipital region), with a dorsally expanded snout; skull width did not show noteworthy variation. DFA on juveniles yielded similar results, with a weaker interspecific distinction (Fig. 4): 13/16 *B. bufo* and 14/17 *B. spinosus* toads were reallocated to their group ($K = 0.63$); T-square test was not significant ($T^2 = 790.5$, $P = 0.72$), while permutation test was significant ($P < 0.0001$).

DISCUSSION

Most of the shape variation in the whole dataset was explained by differences in size, as shown by the concordant results of principal component and regression analyses. Therefore, I suggest that ontogenetic allometry (i.e., the association between morphological changes and ontogenetic growth; Klingenberg, 2016) characterises skull development of both *Bufo bufo* and *Bufo spinosus*, mainly in the form of a considerable widening (typical of skull growth in frogs; Ponssa and Candioti, 2012), and a relative shortening and dorsoventral flattening. Cranial allometry has already been recognized in other anuran species, both in larval (e.g., in *Rana sylvatica*; Larson, 2002) and post-metamorphic development (e.g. in *Rhinella marina* and the *Leptodactylus fuscus* group; Birch, 1999; Ponssa and Candioti, 2012). Allometric constraints are likely to limit phenotypic evolution of the skull, even in presence of selective pressure (Simon et al., 2016). This kind of scenario can be logically applied to the current study, which found shape disparities between

B. bufo and *B. spinosus* that are moderate if compared to the common allometric variation.

Nevertheless, there seems to be a shift in the ontogenetic trajectories of the two species, highlighted by both the principal component analysis (Fig. 2) and the angle between regression vectors (17.2°), and reflected in the morphological distinction provided by the discriminant function analyses (Fig. 4). Along with both latter analyses, T-square test against equal species mean shapes yielded significant results only after permutation, which probably compensated for the relatively small sample size. Interspecific divergence, however, resulted higher in the group of largest individuals: they showed greater agreement to true species membership, as described by a K coefficient of 0.84 against the 0.63 of juveniles. Consequently, it might be easier to discriminate between *B. bufo* and *B. spinosus* at mature stages, rather than among young individuals. This would be in contrast with the findings from other studies on amphibians, which pointed out a decrease in interspecific disparity over ontogeny (Adams and Nistri, 2010; Ponssa and Candioti, 2012).

DFA and, to some extent, PCA, indicate that *B. bufo* toads have on average a longer skull and a more dorsally compressed snout than *B. spinosus* toads. This morphological divergence could theoretically be placed within either the non-allometric or the allometric regime. Variation in non-allometric shape would imply some sort of relaxation of ontogenetic constraints, which seems very unlikely, as the present evidence suggests that these constraints are strong in both species. Alternatively, interpreting interspecific variation as comprised in the allometric framework should better reflect the results of the analyses. Allometric variation could have arisen in two ways. First, from changes in developmental timing of the ancestral shape trajectory, with a conserved shape-size relationship (ontogenetic scaling hypothesis; Strelin et al., 2016); however, this also seems unlikely, because the divergent skull shapes do not correspond to different stages of the same trajectory. Secondly – and more plausibly – divergent evolution of the ontogenetic programme in the two lineages may have occurred, with a conserved direction of early post-metamorphic shape trajectories. The latter hypothesis would imply that interspecific differences have arisen during the long-lasting separation of the lineages (about 9 Ma), and it could even be surprising that they are not more pronounced; as a possible explanation for this moderate divergence, a recent morphological evolution, following rapid postglacial European expansion of *B. bufo* from its Balkan refugium, cannot be excluded (Recuero et al., 2012; Arntzen et al., 2016).

Climate is thought to have an indirect influence on skull morphology, because it determines food type and availability (Simon et al., 2016), and changes in these ecological factors may lead to skull shape divergence – even in closely related species. Alternative climate-driven factors could also induce skull differentiation, such as reproduction sites (water pools) occurrence, and the ability of toads to detect them, which involves the olfactory capsules in the snout region (Trueb, 1993; Simon et al., 2016). Whether such factors are related to the interspecific differences found here – some of which concern the snout, more expanded in *B. spinosus* – it is not possible to say. Arntzen et al. (2013a) hypothesized that in European toads a larger body size, a more pronounced presence of keratinous spines on the cheek warts and a wider head shape might favour defence against predators, namely grass snakes. Although *B. spinosus* apparently meets these requirements more than *B. bufo*, relative cranial width did not show significant interspecific disparity in the current study. Thus, no link was found between widely divergent parotoid glands, a distinctive trait of *B. spinosus*, and a wider skull. Nevertheless, Spined toads could compensate by attaining a wider skull through their bigger size.

For further assessments of drivers and extent of morphological divergence between *B. bufo* and *B. spinosus*, it would be convenient to use a larger sample, especially for adult individuals, in order to properly account for the role of sexual dimorphism and benefit from the highest disparity. Different populations should be considered, since *B. bufo* exhibits remarkable variation across its wide range; for instance, Mediterranean Common toads appear to resemble Spined toads in body size – large – and skin texture – thick and warty (De Lange, 1973; Cvetković et al., 2009; Arntzen et al., 2013a).

ACKNOWLEDGEMENTS

This study was conducted in association with Naturalis Biodiversity Center. I would like to thank Marta Calvo (Museo Nacional de Ciencias Naturales) and Esther Dondorp (Naturalis Biodiversity Center) for access to the material under their supervision, Ana Ivanović for precious suggestions on study design, Rob Langelaan for technical support with computed tomography, and Pim Arntzen and two anonymous reviewers for valuable feedback and remarks on earlier versions of the manuscript.

SUPPLEMENTARY MATERIAL

Supplementary material associated with this article can be found at <http://www.unipv.it/webshi/appendix> manuscript number 24709.

REFERENCES

Adams, D.C., Nistri, A. (2010): Ontogenetic convergence and evolution of foot morphology in European cave salamanders (Family: Plethodontidae). BMC Evol. Biol. **10**: 216.

Arntzen, J.W., McAtear, J., Recuero, E., Ziermann, J.M., Ohler, A., van Alphen, J., Martínez-Solano, I. (2013a): Morphological and genetic differentiation of *Bufo* toads: two cryptic species in Western Europe (Anura, Bufonidae). Contrib. Zool. **82**: 147-169.

Arntzen, J.W., Recuero, E., Canestrelli, D., Martínez-Solano, I. (2013b): How complex is the *Bufo bufo* species group? Mol. Phylogenet. Evol. **69**: 1203-1208.

Arntzen, J.W., Trujillo, T., Butôt, R., Vrieling, K., Schaap, O., Gutiérrez-Rodríguez, J., Martínez-Solano, I. (2016): Concordant morphological and molecular clines in a contact zone of the Common and Spined toad (*Bufo bufo* and *B. spinosus*) in the northwest of France. Front. Zool. **13**: 52.

Birch, J.M. (1999): Skull allometry in the marine toad, *Bufo marinus*. J. Morphol. **241**: 115-126.

Cossu, I.M., Frau, S., Delfino, M., Chiodi, A., Corti, C., Bellati, A. (2018): First report of *Bufo bufo* (Linnaeus, 1758) from Sardinia (Italy). Acta Herpetol. **13**: 43-49.

Cvetković, D., Tomašević, N., Ficetola, G.F., Crnobrnja-Isailović, J., Miaud, C. (2009): Bergmann's rule in amphibians: combining demographic and ecological parameters to explain body size variation among populations in the common toad *Bufo bufo*. J. Zool. Syst. Evol. Res. **47**: 171-180.

Cvijanović, M., Ivanović, A., Kalezić, M.L., Zelditch, M.L. (2014): The ontogenetic origins of skull shape disparity in the *Triturus cristatus* group. Evol. Dev. **16**: 306-317.

De Lange, L. (1973): A contribution to the intraspecific systematics of *Bufo bufo* (Linnaeus, 1758) (Amphibia). Beaufortia **21**: 99-116.

Ivanović, A., Arntzen, J.W. (2018): Evolution of skull shape in the family Salamandridae (Amphibia: Caudata). J. Anat. **232**: 359-370.

Ivanović, A., Sotiropoulos, K., Üzüm, N., Džukić, G., Olgun, K., Cogălniceanu, D., Kalezić, M.L. (2012): A phylogenetic view on skull size and shape variation in the smooth newt (*Lissotriton vulgaris*, Caudata, Salamandridae). J. Zool. Syst. Evol. Res. **50**: 116-124.

Klingenberg, C.P. (2011): MorphoJ: an integrated software package for geometric morphometrics. Mol. Ecol. Resour. **11**: 353-357.

Klingenberg, C.P. (2016): Size, shape, and form: concepts of allometry in geometric morphometrics. Dev. Genes Evol. **226**: 113-137.

Lachenbruch, P.A. (1967): An almost unbiased method of obtaining confidence intervals for the probability of misclassification in discriminant analysis. Biometrics **23**: 639-645.

Larson, P.M. (2002): Chondrocranial development in larval *Rana sylvatica* (Anura: Ranidae): morphometric analysis of cranial allometry and ontogenetic shape change. J. Morphol. **252**: 131-144.

Monteiro, L.R. (1999): Multivariate regression models and geometric morphometrics: the search for causal factors in the analysis of shape. Syst. Biol. **48**: 192-199.

Ponssa, M.L., Candioti, F.V. (2012): Patterns of skull development in anurans: size and shape relationship during postmetamorphic cranial ontogeny in five species of the *Leptodactylus fuscus* Group (Anura: Leptodactylidae). Zoomorphology **131**: 349-362.

Recuero, E., Canestrelli, D., Vörös, J., Szabó, K., Poyarkov, N.A., Arntzen, J.W., Crnobrnja-Isailovic, J., Kidov, A.A., Cogălniceanu, D., Caputo, F.P., Nascetti, G., Martínez-Solano, I. (2012): Multilocus species tree analyses resolve the radiation of the widespread *Bufo bufo* species group (Anura, Bufonidae). Mol. Phylogenet. Evol. **62**: 71-86.

Simon, M.N., Machado, F.A., Marroig, G. (2016): High evolutionary constraints limited adaptive responses to past climate changes in toad skulls. Proc. R. Soc. B Biol. Sci. **283**: 20161783.

Strelin, M.M., Benitez-Vieyra, S., Fornoni, J., Klingenberg, C.P., Cocucci, A.A. (2016): Exploring the ontogenetic scaling hypothesis during the diversification of pollination syndromes in *Caiophora* (Loasaceae, subfam. Loasoideae). Ann. Bot. **117**: 937-947.

Trueb, L. (1993): Patterns of cranial diversity among the Lissamphibia. In: The skull: patterns of structural and systematic diversity, pp. 255-343. Hanken, J., Hall, B.K., Eds, University of Chicago Press, Chicago.

Webster, M., Sheets, H.D. (2010): A practical introduction to landmark-based geometric morphometrics. Paleontol. Soc. Pap. **16**: 163-188.

Zelditch, M.L., Swiderski, D.L., Sheets, H.D., Fink, W.L. (2004): Geometric morphometrics for biologists: a primer. Elsevier/Academic Press, Amsterdam.